Draft version April 24, 2024
Typeset using LaTeX **twocolumn** style in AASTeX631

Implementation of a Time-domain Cosmic-ray-muon Tagger for the NEXUS Low-background Cryogenic Facility

Simon D. Mork [1,2,3] Lauren Hsu [1] Patrick T. Lukens [1] and Dylan J. Temples [1]

[1] *Astrophysics Department, Fermi National Accelerator Laboratory, Kirk & Pine St., Batavia, IL 60510, USA*
[2] *School of Earth and Space Exploration, Arizona State University, 781 Terrace Mall, Tempe, AZ 85287, USA*
[3] *Beus Center for Cosmic Foundations, Arizona State University, 781 Terrace Mall, Tempe, AZ 85287, USA*

ABSTRACT

Quantifying the effects of radiation on the operation of qubits both as quantum information systems as well as particle detectors has emerged as a pressing issue in quantum science in recent years. We present an overview of the design, operation, and deployment of a 90-in^2 three-panel muon detector for use in the NEXUS experimental facility at Fermilab to temporally isolate correlated errors in qubits and determine if they possess an astrophysical origin. Constructed with three scintillator-attached PMTs read out with NIM modules in a triply-coincident logic scheme, we measure a surface-level muon luminosity of 9.7425 muons per second—consistent with an average surface-level cosmic-ray flux of approximately one muon per square centimeter per minute. Integrating the NIM modules with an MCC 128 DAQ HAT and Raspberry Pi, a Python script records exactly when a muon struck the detector and writes a timestamp to a log file for follow-up cross referencing. This experiment will broadly contribute to further studies aimed at understanding the source and mitigation of information loss in qubits.

1. INTRODUCTION

Classical bits underpin all conventional computing technology in use today—where such classical bits represent information in a binary state. However, the concept of binary information is simply a computational idea which can be physically encoded in many different ways. A simple example would be to represent heads as 0 and tails as 1 in a regular coin flip. When the coin lands, there are only two choices for how to interpret the result of the flip. In addition, the process of the flip does not matter at all—all we care about is that the coin is either heads or tails instantaneously. If one wished to build a classical computer out of coin flips, information could only be exchanged between other coins, and thus computing could take place, only after the flip has concluded. Quantum bits, also known as qubits, change the picture by allowing information to be represented as multiple states simultaneously—also known as a superposition. To borrow the coin flip analogy a second time, information can be exchanged between coins *while* they are being flipped. When observed, the coin is still either heads or tails, but the probability of observing heads or tails can be influenced by other coins still actively being flipped. Computing, to be precise, takes place as the wave functions of each qubit evolve continuously instead of discretely as they would in a classical computer.

New chips are being developed that allow engineers and scientists to encode quantum bits into physical systems, similar to how classical computing is built on the encoding of classical bits as either the existence or lack of an electrical charge or pulse in a circuit. Qubits store data much differently than classical bits, and they are susceptible to radiation which create correlated errors that interfere with how they store information (e.g., Martinis 2021; McEwen et al. 2021; Wilen et al. 2021)—much like how a short circuit can damage memory and corrupt information in classical computers. Exploitation of correlated errors which allow qubits to effectively be transformed into particle detectors, particularly in the regime of dark-matter detection, is also possible (e.g., Linehan et al. 2024). The testing and operation of quantum chips benefits greatly from low-background facilities where the rate of background radiation is many orders of magnitude lower than that of a surface-level facility.

NEXUS is a 360 ft^2 space located adjacent to the MINOS excavated cavern at Fermilab with a 107 meter rock overburden (e.g., Michael et al. 2008). The clean room at NEXUS contains a movable lead shield which shields a dilution refrigerator that acts as a testbed for low-background calibration and science with superconducting dark-matter detectors (e.g., Temples et al. 2024). While the significant rock overburden substantially reduces the flux of surface-level background-

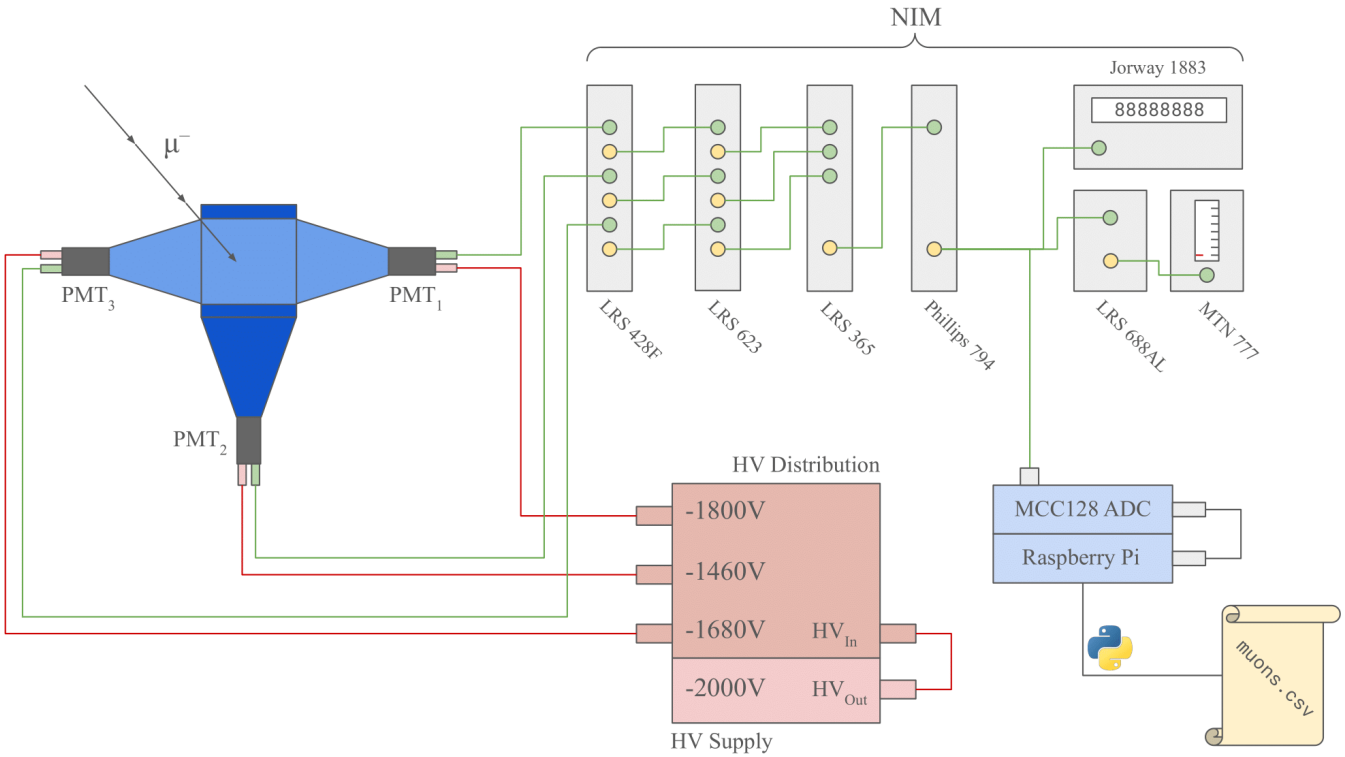

Figure 1. A block diagram of the entire muon detection-and-digitization system. Scintillator paddles are depicted as blue rectangles and waveguides as the attached blue trapezoids. PMTs (tubes and bases) are depicted as gray rectangles attached to the blue waveguides. High-voltage cables are denoted as red lines and low-voltage signal cables are denoted as green lines. Logical connections between the DAQ and Pi along with the final data product are denoted as gray lines. Channel input/output(s) are denoted as green and yellow circles respectively on the NIM modules. Only the actively utilized NIM modules along with their associated input/output channel(s) used in the current detection system are shown here for visual clarity. The three branching signal cables running from the output of the Phillips 794 module indicate that it may be routed to any one of the three possible output routes. Scintillator and PMT paddle dimensions are not to scale.

radiation products from cosmic-ray spallation, it does not eliminate all of it—particularly muons. Cosmic rays present a major challenge to operating highly sensitive qubits, as they deposit large amounts of energy in any matter they pass through and can create correlated errors in current qubit designs (e.g., Harrington et al. 2024). Exploring cosmic-ray-induced errors at NEXUS will to contribute to an overarching need to understand the most damaging types of radiation on qubit operation and devise mitigation strategies for quantum computing. In addition, it has the potential to further quantify qubit sensitivity for the purposes of using them as particle detectors. To cross-reference errors in a given chip with cosmic rays, we design and construct a detector that will be deployed adjacent to the refrigerator to tag such cosmic rays as shown in Figure 1.

2. DESIGN

At the heart of the cosmic-ray detection system lies two 1-cm-thick scintillators and one 2-cm-thick scintillator that together act as the main detectors shown in Figure 2. A scintillator is a special kind of material that, when struck with high-energy photons or particles, such as muons or neutrons, emits lower-energy photons. When the three scintillators are stacked on top of one another, the overlapping surface area between the three scintillators is a roughly square 90 in^2. Each of the scintillators are connected to a photomultiplier tube (PMT) which enables the collection of scintillation light emitted by a muon collision. The PMT itself consists of a photocathode which is charged to a negative high-voltage bias that converts an incoming scintillation photon to a photoelectron via the photoelectric effect. This electron collides with a cascading ladder of dynodes which are charged to an increasingly lower negative bias voltage. Each collision by an electron to one of the dynodes creates a cascade of secondary electrons which each go on to collide with the next dynode in the array, thus exponentially multiplying the signal of the initial input photon. The negative high-voltage bias applied to the PMT photocathode and dynodes is supplied by a high-voltage distribution system in a two-step process. High-voltage

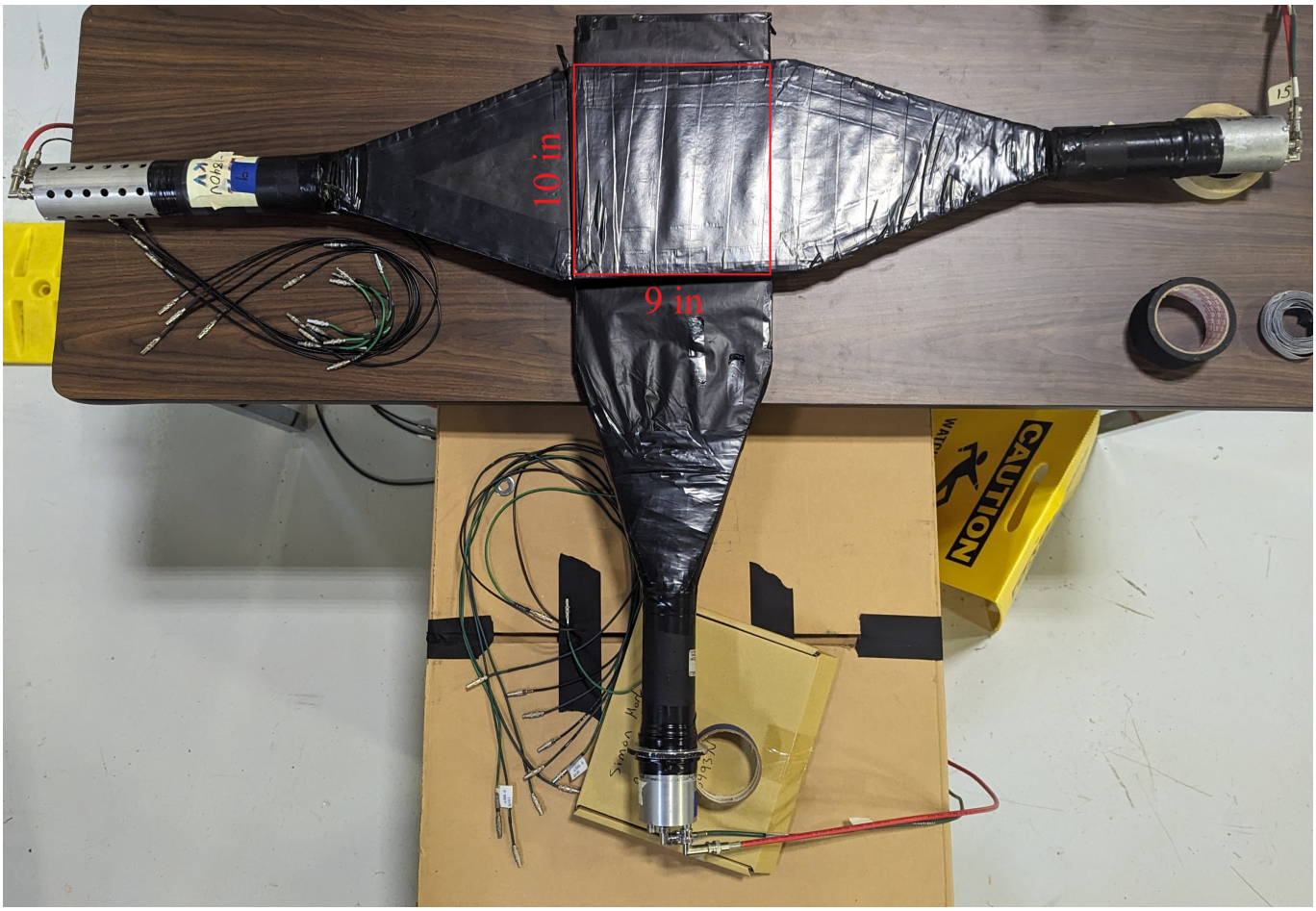

Figure 2. A photo of the three scintillator paddles used in the detection system with their attached waveguides and PMTs. The 9 x 10 in surface area in which all three muon paddles overlap is shown as a red box labeled with its respective dimensions.

is first supplied by a single high-voltage power supply at a voltage of −2000V. This single high-voltage line is then sent to a multi-channel distribution box which steps down the input voltage in +20V increments per-channel in order to send a custom high-voltage bias to each PMT. Three high-voltage lines carry the power from three channels on the distribution box to the base of each PMT. Coaxial cables finally carry the signal from the PMT anode to a NIM crate containing a variety of NIM modules that together generate a logic pulse whenever a triply coincident pulse in the PMTs is detected.

The need for such a triply coincident event across three separate scintillators is because the PMTs trigger on more than just muons. We are also concerned with background radiation and dark current that generate signal in the PMTs. Naturally present gamma rays from background radiation have the potential to generate coincident scintillation photons in the scintillators. However, the chance that a given gamma ray will hit and generate a detection in all three scintillators is substantially lower than the chance that it will hit just one or two of them—hence why we have implemented three scintillator paddles into our detection system. In addition, a dark current of tens or hundreds of Hz (or more) may be observed in each of the scintillators as the photocathode spontaneously emits photoelectrons. Enforcing that only triply-coincident pulses detected in the scintillators are tagged as an event allows us to subtract the uncorrelated dark noise from the measurement and retain the genuine genuine cosmic-ray signal. The rate of dark current is a strongly nonlinear function of the PMT bias voltage, meaning that the dark current rate goes up exponentially as the PMT is biased to an increasingly higher voltage. During the calibration phase of the detector setup, the voltage was chosen to be as low as possible across all three PMTs while still recovering a reasonable surface-level flux of muons to eliminate the probability of a stochastic triply-coincident event being falsely logged as a real event. This probability is goverened by Poisson statistics, and calculating the probability of such a triply-coincident event purely from random chance is straightforward.

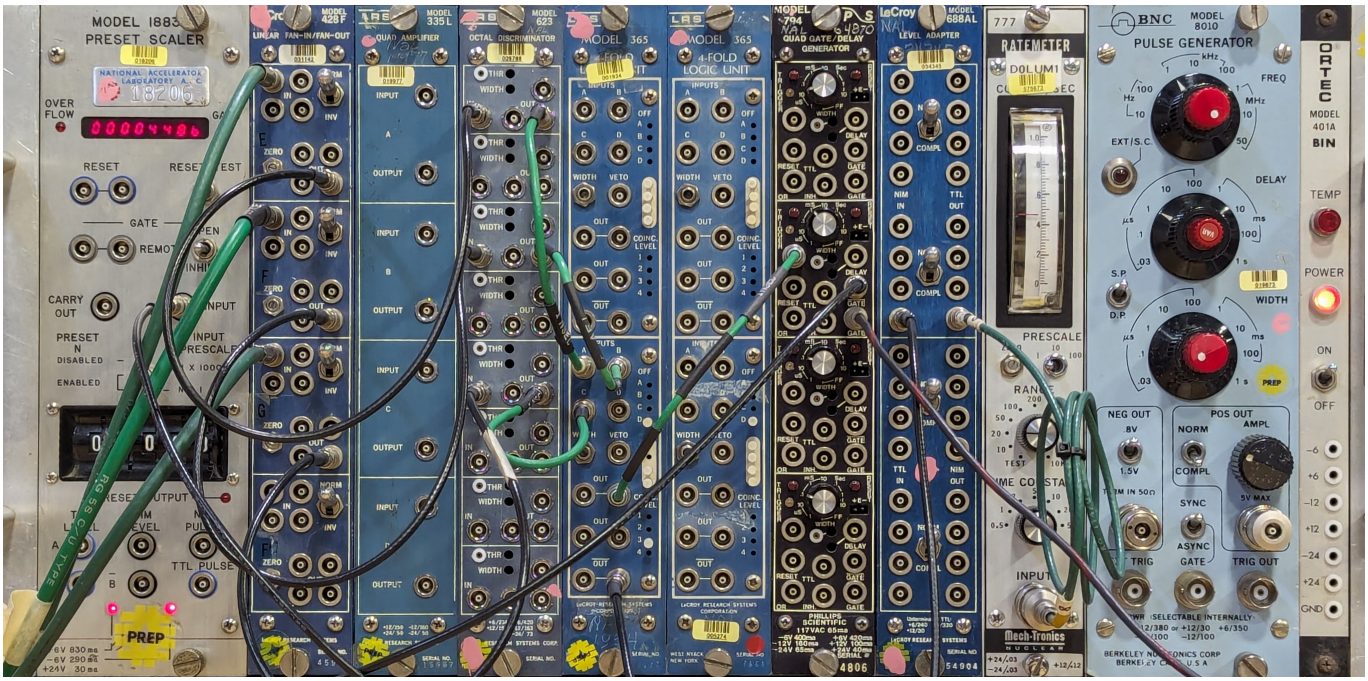

Figure 3. A photo of the front panel of the NIM modules used to detect muon collisions in the scintillators. From left to right, the modules are as follows: Jorway 1883*, LRS 428F, LRS 335L, LRS 623, LRS 365, LRS 365, Phillips 794, LRS 688AL, MTN 777, BNC 8010*. Asterisks denote double-width modules. See Appendix A for more information.

$$P(k \text{ events in interval } t) = \frac{(rt)^k e^{-rt}}{k!} \tag{1}$$

$$P(1 \text{ false event in } T) = 1 - \left(1 - \frac{(rt)^k e^{-rt}}{k!}\right)^n \tag{2}$$

$$P(1 \text{ false event in } T) \approx \frac{T(rt)^k e^{-rt}}{t(k!)} \tag{3}$$

To quantify the chance that a stochastic coincidence occurs, we evaluate Equation 3 where r is the sum of the pulse rate from the three discriminator channels (500 Hz), t is the coincidence window set by the discriminator logic pulse width (10 ns), k is the coincidence threshold (3), and n is the number of coincidence windows in some larger scan time T. For $T = 1$ minute, $n = 6 \times 10^9$. Accounting for proper unit conversions, the evaluation of Equation 3 nets us a probability of 1.25×10^{-7}. In other words, only one false coincidence, on average, every 15.22 years. While this approximation incorrectly assumes that the full 500 Hz of combined signal is from uncorrelated dark current, it is an order-of-magnitude approximation which signifies that the detector will be free of dark-current false positives.

The coincident logic pulse is then digitized and written to a .csv file that records the time of detection for the muon collision in the scintillators. Post-acquisition, this file is used as a cross-reference to glean the source of events detected in the qubits or dark matter detectors present in the NEXUS refrigerator.

3. OPERATION

When cosmic rays pass through the rectangular scintillators, they deposit energy as they collide with the crystalline structure of the plastic. This energy is converted to scintillation photons which are radiated isotropically from the point of collision. These photons then propagate through the bulk of the plastic and are reflected by a light-tight reflective wrapping around the scintillator until they encounter a plastic waveguide that directs the scintillation photons to the photocathode of the PMT.

When read on an oscilloscope, the resulting signal from the PMT appears as a pulse with a fast rise time of $\mathcal{O}(1)$ ns and exponential decay time of $\mathcal{O}(10)$ ns, both scaling slightly larger depending on the amplitude of the pulse. The larger the energy deposit in the scintillator, the more scintillation photons that are created, and thus the larger the amplitude of the resulting signal pulse. These signals are then sent to a rack of NIM modules as shown in Figure 3 for analysis.

The signal output of the three PMTs is first used as the input to a Lecroy Model 428F Linear Fan-in/Fan-out module. This allows us to read out the PMT pulses while simultaneously sending the signal to the rest of detection electronics if needed for calibration or future upgrades. In order to convert the incoming signal pulses into NIM-standard logic pulses, we then use the output of the Fan-in/Fan-out on each channel as the in-

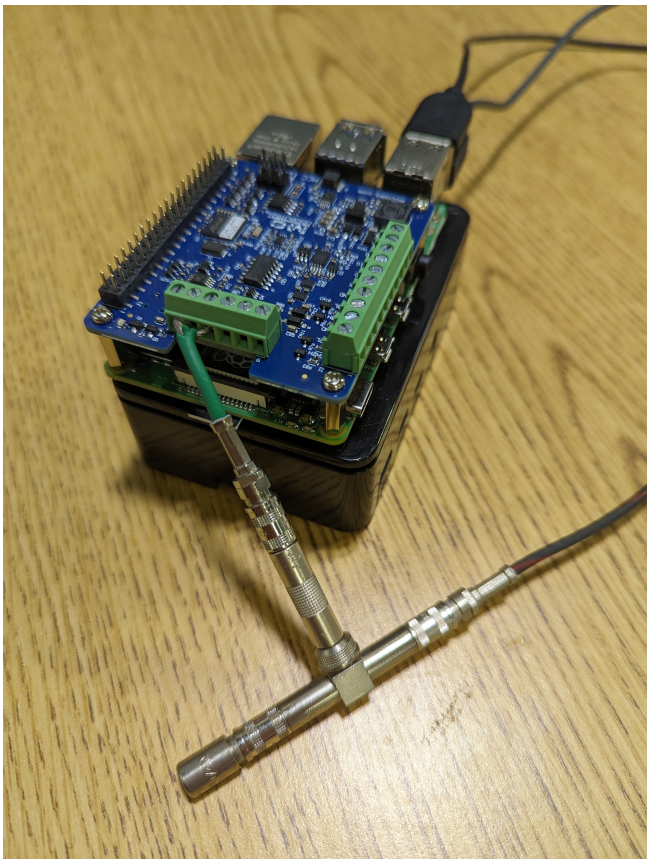

Figure 4. A photo of the MCC 128 DAQ HAT with a 50Ω-terminated LEMO from the Phillips 794 being fed to Channel 0 of the DAQ.

Figure 5. A photo of the lead shield encapsulating the dilution refrigerator used in NEXUS. The scintillators will lay inside the shield below the refrigerator.

put to a LeCroy Model 623 Octal Discriminator module. The discriminator first scans for a falling-edge pulse at a custom-set threshold of −30mV, then sends out a square-wave logic pulse with an amplitude of ≈ −800mV and custom-set full-width-at-half-maximum (FWHM) of 10 ns if the threshold criteria was met.

The logic pulses from the discriminator are then used as the input to a LeCroy Model 365 4-fold Logic Unit module. The logic unit allows us to take the logic pulses from the three discriminator channels and determine how many scintillators flashed within a coincidence time window set by the width of the discriminator pulses—in our case, 10ns. Even with perfectly-calibrated signal cable lengths and electronic delay, there is natural jitter in the arrival time of muon pulses to the electronics as a function of the geometry of the experiment. A 10 ns coincidence window was chosen to minimize the chance of logging a dark-current stochastic-coincidence false event while maximizing the efficiency of genuine detections from this natural jitter. Set at the triply-coincident threshold level, the logic unit then generates another custom-width NIM pulse whenever such a coincidence is detected. With NIM pulses for genuine cosmic rays, the next step is to digitize them.

An MCC 128 DAQ HAT board was procured which interfaces with a CanaKit Raspberry Pi to provide 8-channel analog-to-digital converter (ADC) capabilities with a maximum readout frequency bandwidth of 100 kilosamples per second (kS/s). In its highest-frequency mode, the MCC 128 samples the analog voltage every 10,000 ns. However, we are limited by the fact that data acquired in the 100 kS/s mode must be read out of the onboard memory buffer with approximately 2-5% downtime relative to the total length of acquisition time. While this nets us great timing resolution, we lose time in which the signal line voltage is not being monitored as the voltage samples are read out of memory. Therefore, we instead choose to operate the MCC 128 in a continuous acquisition mode where the time between samples is no longer constant but rather takes on a distribution of times centered on ≈115 μs. Repeated testing found that $> 99.5\%$ of the time between samples in this mode were $< 200\mu$s. Therefore, while we lose a factor of 20 in timing resolution, we minimize the downtime of the de-

tection system by a similar factor. In addition, because the response time of the detectors alongside which this detection system will run are relatively slow, a higher uptime was viewed as more desirable relative to the loss in timing resolution.

Because the logic signals created by the Lecroy Model 365 only have a pulse width of 20 ns, sampling at an average rate of 115 μs would fail to digitize virtually all detected cosmic rays. To solve this problem, we make use of the Phillips Model 794 Quad Gate/Delay Generator to generate a NIM logic pulse of arbitrary width whenever it is triggered by an external NIM logic pulse. By setting it to generate a pulse with a width of 200 μs, we feed this logic output to Channel 0 of the MCC 128 DAQ HAT to digitize the logic pulse as shown in Figure 4. With a custom Python script (see Appendix B) that monitors the signal voltage for pulses, we write the current time to a log file each time that the script detects a signal with a timing resolution set by the pulse width of the Phillips 794. Since the scope of the detection system is only to measure the time-of-collision for a muon collision at NEXUS, we only digitize the logic pulses and do not digitize the PMT pulses themself.

Optionally, the output of the Fan-in/Fan-out module may be shunted to the input of a Lecroy Model 335L Quad 6x Amplifier module in order to increase the gain of our PMTs without increasing the dark current via further biasing the photocathode. However, this vastly increases the chance of a stochastic coincidence without further downbiasing of the PMTs, and this is left as a future upgrade path for the detection system. The output of the gate generator may also be shunted to the input of a Lecroy Model 688AL Bi-directional NIM-TTL Logic Translator module in order to translate the negative NIM logic pulses to positive TTL logic pulses. These positive pulses can then be read by a Mech-tronics Nuclear Model 777 Ratemeter to achieve realtime visualization of the active rate of cosmic rays being detected by the scintillators—or for other purposes. The output of the gate generator may also be directly shunted to the input of a Jorway Model 1883 Visual Scaler and Preset Pulse Generator for a visually readable running tally of the detected cosmic rays.

4. RESULTS

After operating the detector for 7,545 seconds, we counted 73,507 detections as read out by the LRS 365 and counted by the Jorway 1883. From this, we calculate an incident muon luminosity of of 9.7425 μ^- s^{-1}. Using this luminosity, we calculate that the observed flux, assuming an operational detection area of 9 x 10 in, is ≈ 1 μ^- cm^{-2} min^{-1} using Equations 4 and 5. This is in agreement with Autran et al. (2018).

$$9.7425 \ \frac{\mu^-}{\text{s}} \cdot \frac{1}{9 \text{ in}} \cdot \frac{1}{10 \text{ in}} \approx 0.1083 \ \frac{\mu^-}{\text{in}^2 \text{ s}} \tag{4}$$

$$0.1083 \ \frac{\mu^-}{\text{in}^2 \text{ s}} \left(\frac{1 \text{ in}}{2.54 \text{ cm}} \right)^2 \frac{60 \text{ s}}{1 \text{ min}} \approx 1 \ \frac{\mu^-}{\text{cm}^2 \cdot \text{min}} \tag{5}$$

5. CONCLUSION AND FURTHER WORK

We have successfully implemented a design for a muon tagger for the NEXUS facility using legacy hardware at Fermilab with a material cost of $< \$400$ and have recovered a theoretically plausible surface-level muon flux; the detection system will be deployed at the NEXUS underground facility in the coming months as of the date of this draft. The three muon paddles will be placed together inside of a movable lead shield that encloses the dilution refrigerator at NEXUS. Laying at the bottom of this shield, the three paddles will detect any muons that pass through detectors inside of the refrigerator.

Also undertaken as a part of this internship was an upgrade to the NEXUS lead shield itself, shown in Figure 5, encompassing the refrigerator. As a part of upgrades to the lead shield, lead bricks were stacked an additional three vertical feet on all three walls of the shield in order to increase the height of the shield to its full experimental limit. In addition, a horseshoe-shaped lead collar which encloses the top of the shield to create a fully-shielded volume for the dilution refrigerator was raised three feet and properly aligned. Additional support electronics and mechanical changes were implemented in order to keep readout electronics at the top of the refrigerator from interfering with normal opening and closing of the lead shield in its new state.

Future work may involve acquiring a fourth scintillator paddle and bifurcating the detection system into a top section and a bottom section. The top section would be placed above the NEXUS refrigerator, and the bottom section would be placed in the movable lead shield as normal. This would further restrict the acceptance angle of muons into the detectors to only those from directly above the system. The NIM modules already contain room for a fourth channel to accommodate this upgrade, and such an upgrade should be possible as soon as a suitable scintillator paddle can be acquired and the requisite time spent upgrading the acquisition script, NIM wiring, and refrigerator superstructure.

ACKNOWLEDGMENTS

Simon Mork would like to thank his supervisor, Lauren Hsu, in addition to Patrick Lukens, Dylan Temples, and Dan Baxter for all of the guidance they provided him during his SULI internship. In addition, he would

like to thank them for fostering a welcoming environment at Fermilab for an early-career scientist who was initially unexposed to the field of particle physics and quantum science upon entering Fermilab.

This manuscript has been authored by Fermi Research Alliance, LLC under Contract No. DE-AC02-07CH11359 with the U.S. Department of Energy, Office of Science, Office of High Energy Physics. This work was supported in part by the U.S. Department of Energy, Office of Science, Office of Workforce Development for Teachers and Scientists (WDTS) under the Science Undergraduate Laboratory Internships Program (SULI).

Software: `daqhats` (MCC 2023) `matplotlib` (Hunter 2007), `numpy` (Harris et al. 2020), `pandas` (Wes McKinney 2010).

REFERENCES

Autran, J., Munteanu, D., Saad Saoud, T., & Moindjie, S. 2018, Nuclear Instruments and Methods in Physics Research Section A: Accelerators, Spectrometers, Detectors and Associated Equipment, 903, 77, doi: https://doi.org/10.1016/j.nima.2018.06.038

Harrington, P. M., Li, M., Hays, M., et al. 2024, Synchronous Detection of Cosmic Rays and Correlated Errors in Superconducting Qubit Arrays. https://arxiv.org/abs/2402.03208

Harris, C. R., Millman, K. J., van der Walt, S. J., et al. 2020, Nature, 585, 357, doi: 10.1038/s41586-020-2649-2

Hunter, J. D. 2007, Computing in Science & Engineering, 9, 90, doi: 10.1109/MCSE.2007.55

Linehan, R., Hernandez, I., Temples, D. J., et al. 2024, Estimating the Energy Threshold of Phonon-mediated Superconducting Qubit Detectors Operated in an Energy-Relaxation Sensing Scheme. https://arxiv.org/abs/2404.04423

Martinis, J. M. 2021, npj Quantum Information, 7, doi: 10.1038/s41534-021-00431-0

MCC. 2023, daqhats, https://github.com/mccdaq/daqhats, GitHub

McEwen, M., Faoro, L., Arya, K., et al. 2021, Nature Physics, 18, 107–111, doi: 10.1038/s41567-021-01432-8

Michael, D., Adamson, P., Alexopoulos, T., et al. 2008, Nuclear Instruments and Methods in Physics Research Section A: Accelerators, Spectrometers, Detectors and Associated Equipment, 596, 190, doi: https://doi.org/10.1016/j.nima.2008.08.003

Temples, D. J., Wen, O., Ramanathan, K., et al. 2024, Performance of a Kinetic Inductance Phonon-Mediated Detector at the NEXUS Cryogenic Facility. https://arxiv.org/abs/2402.04473

Wes McKinney. 2010, in Proceedings of the 9th Python in Science Conference, ed. Stéfan van der Walt & Jarrod Millman, 56 – 61, doi: 10.25080/Majora-92bf1922-00a

Wilen, C. D., Abdullah, S., Kurinsky, N. A., et al. 2021, Nature, 594, 369–373, doi: 10.1038/s41586-021-03557-5

APPENDIX

A. HARDWARE

Table 1. Hardware used in the Detection System

Quantity	Manufacturer	Model	Description
1	Ortec	401A*	NIM Bin
1	Jorway	1883*	Visual Scaler and Preset Pulse Generator
1	LRS	428F	Linear Quad-channel Fan-in/Fan-out
1	LRS	335L*	6x Quad-channel Linear Amplifier
1	LRS	623	Custom-threshold Octal Discriminator
2	LRS	365	Quad-channel Arbitrary-coincidence Unit
1	Phillips	794*	Quad-channel Gate/Delay Generator
1	LRS	688AL	Bi-directional NIM-TTL Logic Translator
1	MTN	†777*	1Hz–1Mhz Visual Ratemeter
1	BNC	8010*	Arbitrary Logic Pulse Generator
1	Power Designs	HV1547*	High-Voltage Power Supply
1	Fermi	11X2562SIC*	High-Voltage Zener Divider
1	MCC	128	Analog-to-Digital Voltage Sampler
1	CanaKit	Raspberry Pi - 8GB	Python Watchdog Script Executor
4			High-Voltage Cable
17			LEMO Signal Cable

NOTE—Abbreviations used in the text are as follows: BNC/Berkeley Nucleonics Corporation. Fermi/Fermilab. LRS/Lecroy/Lecroy Research Systems. MCC/Measurement Computing Corporation. MTN/Mech-Tronics Nuclear. Phillips/Phillips Scientific. Asterisks denote links only accessible via Fermilab authentication. †Links to a similar, but not quite the same, module due to a lack of online documentation for the exact module used.

B. SOFTWARE

The Python script written to monitor the NIM logic voltage for muon detections may be found here: https://github.com/CosmiQuantum/muon-monitor-rpi